JOURNAL OF CATALYSIS 120, 337–352 (1989)

Nickel-Loaded $K_4Nb_6O_{17}$ Photocatalyst in the Decomposition of H_2O into H_2 and O_2: Structure and Reaction Mechanism

A. KUDO, K. SAYAMA, A. TANAKA,* K. ASAKURA,† K. DOMEN, K. MARUYA, AND T. ONISHI[1]

*Research Laboratory of Resources Utilization, Tokyo Institute of Technology, 4259 Nagatsuta, Yokohama 227; *Nikon Company, 1773 Asamizodai, Sagamihara 228; †Faculty of Science, The University of Tokyo, 7-3-1 Hongo, Bunkyo-ku, Tokyo 113, Japan*

Received March 1, 1989; revised July 6, 1989

The structure of nickel-loaded $K_4Nb_6O_{17}$ photocatalyst in an overall water splitting reaction was studied by means of XPS, EXAFS, TEM, and XRD. $K_4Nb_6O_{17}$ has an ion-exchangeable layered structure which possesses two different kinds of alternating interlayer spaces, i.e. interlayers I and II, where K^+ ions are located. The interlayers are hydrated in an aqueous solution. It was revealed that in the active catalyst which was pretreated by H_2 at 773 K for 2 h and reoxidized by O_2 at 473 K for 1 h, loaded nickel is predominantly located in interlayer I as ultrafine metal particles (ca. 5 Å). In contrast, only a very small amount of nickel was observed over the external surface of $K_4Nb_6O_{17}$. On the basis of the structure, a novel mechanism for the photodecomposition of H_2O into H_2 and O_2 is proposed; i.e., intercalated water is reduced to H_2 in interlayer I and is oxidized to O_2 in interlayer II. Therefore, each niobate macroanion sheet is regarded as a "two-dimensional" photocatalyst where H_2 and O_2 evolve at different sides of the layer.

INTRODUCTION

The photodecomposition of water has been extensively studied on various systems (*1*); however, a sustained and overall water splitting into H_2 and O_2 has been accomplished in only a limited number of cases (*2–6*). Most of these systems use semiconductor particle based-photocatalysts. An accepted reaction mechanism in general seems to be based on a photo-produced electron-hole pair separation. This is caused by an electronic band structure of the semiconductor interface with a solution. It is the mechanism which was originally designated for a semiconductor photoelectrode (*7*). At the present stage, however, the quantum efficiency (qe) for an overall water splitting is still very low (qe $\leq$ 1%) over such a semiconductor particle photocatalyst, while high qe (>50%) is often obtained by the addition of a so-called "sacrificial reagent." This suggests that photo-excited electrons and holes can be well separated in a small semicondutor particle and that they are available at least for an irreversible chemical reaction. It is, therefore, inferred that a low efficiency of photodecomposition of water into H_2 and O_2 is mainly due to a rapid back-reaction between products and/or reaction intermediates over a small particulate system (*8*). Thus, a critical problem to be accomplished for an efficient up-hill reaction is to prevent such a thermodynamically favored back-reaction.

Recently we have reported that $K_4Nb_6O_{17}$ loaded with nickel is a novel photocatalyst for the decomposition of water into H_2 and O_2 (*5*). It has also been found that the $K_4Nb_6O_{17}$ photocatalyst has several remarkable differences from catalysts based on other semiconductor particles such as TiO_2 and $SrTiO_3$. As for the structure of this material it is known that $A_4Nb_6O_{17}$ (A = K, Rb, Cs) are layered compounds (*9*), and A^+ ions are replaced by various cations (*10, 11*). Gasperin and Le Bihan have clari-

[1] To whom correspondence should be addressed.

0021-9517/89 $3.00

fied the structures of some of these compounds (*9*). According to their results, corrugated niobate sheets are stacked along the *b*-axis of an orthorhombic unit cell and form four interlayer spaces which are classified into two types. It is also known that alkali ions are distributed in these spaces. The first interlayer space (denoted as interlayer I) has a capacity to take up water molecules, but the second layer (interlayer II) is not hydrated under ambient conditions. Kinomura *et al.* investigated ion-exchange reactions of $K_4Nb_6O_{17} \cdot nH_2O$ with Li^+, Na^+, Ca^{2+}, and Ni^{2+} ions (*11*). They found that K^+ ions were replaced by Li^+ and Na^+ ions in both interlayers I and II while Ni^{2+} ions replaced K^+ ions only in interlayer I. It is notable that interlayer II, where the K^+ ions were replaced by Li^+ or Na^+ ions, was also hydrated in aqueous solution.

According to our previous work (*5*), $K_4Nb_6O_{17}$ immersed in distilled water itself exhibited an activity of simultaneous evolution of H_2 and O_2 under the band gap (3.3 eV) irradiation, although the amount of evolved O_2 was ca. 20% of the stoichiometric ratio. Among the members of a series of $K_4Nb_6O_{17}$ catalysts modified by various transition metals, a marked increase in the activity and stoichiometric evolution of H_2 and O_2 resulted from nickel-loaded $K_4Nb_6O_{17}$ prepared by an impregnation method followed by a proper pretreatment (*5*).

Some other remarkable features of the catalysts are as follows:

(1) The optimum activity is obtained when 0.1 wt% of nickel is loaded as NiO. Below 0.1-wt% loading the activity increases almost proportionally with the increase of loading amount, and above 0.1 wt% the activity decreases gradually.

(2) To activate the catalyst, $K_4Nb_6O_{17}$ impregnated in aqueous $Ni(NO_3)_2$ solution is normally reduced by H_2 at 773 K (R773) and reoxidized by O_2 at 473 K (O473). The quantum efficiency of the R773-O473 NiO (0.1 wt%)–$K_4Nb_6O_{17}$ catalyst was ca. 3.5% at 330 nm (*5*). Even over the catalyst reduced at 773 K, H_2 and O_2 evolve in almost stoichiometric ratio. This result is in contrast to that of $SrTiO_3$-based photocatalyst which was reported previously (*3*). Under the same pretreatment condition, Ni–$SrTiO_3$ photocatalyst evolved a small amount of H_2 and no O_2, and nickel over $SrTiO_3$ was oxidized during irradiation.

(3) Reverse reaction from evolved H_2 and O_2 to form H_2O is negligible under the reaction condition.

(4) The activity of photocatalytic decomposition of water decreases in the concentrated KOH solution (pH > 11), which is a favorable condition for $SrTiO_3$- or TiO_2-based photocatalysts (*2–4, 6*).

The purpose of the present study is to elucidate the relationship between the characteristic behavior and the catalyst structure of an active nickel-loaded $K_4Nb_6O_{17}$. Furthermore, the reaction mechanism of the photocatalytic evolution of H_2 and O_2 is discussed.

To determine the catalyst structure at various stages of the pretreatment, X-ray photoelectron spectroscopy (XPS), extended X-ray absorption fine structures (EXAFS), transmission electron microscopy (TEM), and X-ray diffraction (XRD) measurements were carried out.

EXPERIMENTAL

$K_4Nb_6O_{17}$ and $KNbO_3$ powders were prepared from Nb_2O_5 (Mitsui Kinzoku) and K_2CO_3 (Asahi Glass Co.) at 1573 K for 15 min in air, and the crystal structures were confirmed by X-ray diffraction (XRD). Nickel-loaded $K_4Nb_6O_{17}$ was prepared by impregnation of $K_4Nb_6O_{17}$ powder with an aqueous $Ni(NO_3)_2$ solution (4 ml). The solution was dried, and the catalyst obtained was calcined at ca. 550 K in air for 1 h. The catalyst at this stage is referred to as the "untreated" catalyst. The catalyst was then treated in a closed gas circulation system. A typical treatment was performed first by H_2 reduction at 773 K for 2 h

("R773" catalyst) and then by O_2 oxidation at 473 K for 1 h ("R773-O473" catalyst). $K_4Nb_6O_{17}$ was hydrated and changed into $K_4Nb_6O_{17} \cdot nH_2O$ (n = 3, 4.5, or more) under the reaction conditions. In this paper, however, the catalyst is described as "$K_4Nb_6O_{17}$" and nickel-loaded catalysts are usually indicated as "NiO–$K_4Nb_6O_{17}$" for convenience. Yet, the supported nickel does not always exist as NiO after every treatment, which becomes clear in the present study as shown below.

EXAFS measurements were carried out by using EXAFS apparatus at beam line 10B with synchroton radiation emitted from the Photon Factory at the National Laboratory for High Energy Physics (KEK-PF) (*12*). The catalyst was mixed with polyethylene or boron nitride to form a disk for an EXAFS sample and was exposed to air during the measurement for ca. 1 h.

XPS measurements were conducted by a Shimadzu spectrometer ESCA750. Each treated sample was mounted on a sample holder in an Ar-filled glovebox without air contact. Ar was evaporated over the sample, and the binding energies were corrected using a Au $4f_{7/2}$ peak at 83.8 eV.

Although the most active catalyst was obtained at 0.1 wt% loading of NiO, the catalyst of 1 wt% loading was used for XPS and EXAFS measurements because of the sensitivity problem of those spectroscopic techniques.

TEM photographs were obtained by JEM-2000FX, -2000EX (JEOL), or EM-002B/UHR (Akashi Beam Technology).

XRD patterns were measured by a instrument of Rigaku (30 kV, CuKα, 15 mÅ, 2°/min).

RESULTS

(*1*) *Activities of Variously Treated Ni-Loaded $K_4Nb_6O_{17}$ Photocatalysts*

The rates of H_2 and O_2 evolution in distilled water over variously pretreated nickel-loaded $K_4Nb_6O_{17}$ catalysts, the structures of which were examined in this study, are summarized in Table 1. Similar and more detailed results of activities of $K_4Nb_6O_{17}$-based photocatalysts have been reported elsewhere (*5*). The most active catalyst was obtained by R773-O473 pretreatment of NiO(0.1 wt%)–$K_4Nb_6O_{17}$, and the R773 catalyst also showed relatively high rates of H_2 and O_2 evolution in stoichiometric ratio. The activities of NiO(1 wt%)–$K_4Nb_6O_{17}$ were lower by a factor of about 2 than those of NiO(0.1 wt%)–$K_4Nb_6O_{17}$ for R773 and R773-O473 treatments, respectively. For the R773 NiO(1 wt%)–$K_4Nb_6O_{17}$, the amount of evolved O_2 was considerably smaller than half the amount of the evolved H_2. When the amount of loaded nickel was increased, such as in R773-O473 NiO(20 wt%)–

TABLE 1

Activities of Photodecomposition of Water over Variously Treated NiO–$K_4Nb_6O_{17}$ Catalysts

Catalyst	Activity (μmol/h)	
	H_2	O_2
NiO(0.1 wt%)–$K_4Nb_6O_{17}$		
Untreated[a]	4	1
R773[b]	59	28
R773-O473[c]	73	36
R773-O773[d]	4	1
NiO(1 wt%)–$K_4Nb_6O_{17}$		
Untreated	3	1
R773	31	10
R773-O473	40	18
R773-O773	10	3
NiO(20 wt%)–$K_4Nb_6O_{17}$		
R773-O473	1	0

Note. Activities were determined from the reaction time courses for 10-h high-pressure mercury lamp (450 W) inner irradiation-type reaction cell.

[a] Untreated: after calcination at ca. 550 K in air.

[b] R773: H_2 reduction at 773 K for 2 h.

[c] R773-O473: O_2 oxidation at 473 K for 1 h after R773.

[d] R773-O773: O_2 oxidation at 773 K for 1 h after R773.

$K_4Nb_6O_{17}$, the photocatalytic activity of water decomposition almost disappeared. The untreated and R773-O773 photocatalysts showed very low activities.

Another characteristic behavior of this catalyst is that the rate of H_2O decomposition is insensitive to the presence of gaseous O_2. In Fig. 1, the effect of gaseous O_2 of 300 Torr on the photodecomposition of H_2O over the R773-O473 NiO(0.1 wt%)–$K_4Nb_6O_{17}$ catalyst is shown. The same rates of H_2 evolution from distilled water under both Ar and O_2 atmospheres were obtained within the range of experimental error.

From these results, it is clear that the activity of this catalyst is very sensitive to the amount of loaded nickel and the pretreatment condition. To reveal the reason for the characteristic behavior of this catalyst, the following structural studies were conducted.

(2) *XPS and Chemical Analysis*

For NiO(0.1 wt%)– and NiO(1 wt%)–$K_4Nb_6O_{17}$ catalysts, 0.66 and 6.6% of total K^+ ions are replaced by Ni^{2+} ions, respectively, if all Ni^{2+} ions are intercalated to compensate the electronic charge balance. An atomic absorption measurement showed that expected amounts of Ni and K existed in both "untreated" samples within the experimental error. This indicated that the amount of exchange between K^+ ions and H^+ or H_3O^+ ions in aqueous solution (4 ml) was trivial (at most 5% of total K^+ ions) during the impregnation procedure.

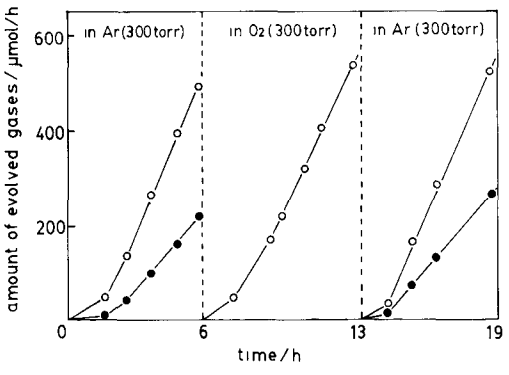

FIG. 1. The effect of gaseous O_2 on the photodecomposition of H_2O over R773 NiO(0.1 wt%)–$K_4Nb_6O_{17}$. (○) H_2 evolved, (●) O_2 evolved. The reaction at 0–6 h and 13–19 h was carried out under 300 Torr of Ar and the reaction at 6–13 h under 300 Torr of O_2.

TABLE 2

XPS Peak Intensity Ratio of Ni2$p_{3/2}$/Nb3d

Catalyst	Peak ratio of Ni2$p_{3/2}$/Nb3d			
	Untreated	R773	R773-O473	R773-O773
NiO(1 wt%)–$K_4Nb_6O_{17}$	0.026	0 004	0.004	0 05
NiO(1 wt%)–$KNbO_3$	1 5	0 7	1 4	1 3
$NiNb_2O_6$	0 6			

XPS measurements were carried out only for NiO(1 wt%)–$K_4Nb_6O_{17}$ but not for NiO (0.1 wt%)–$K_4Nb_6O_{17}$ because of the relatively low sensitivity. NiO(1 wt%)–$KNbO_3$ and $NiNb_2O_6$ were also studied as references. Both $KNbO_3$ and $NiNb_2O_6$ references have BET surface areas (ca. 1 m^2/g) similar to that of $K_4Nb_6O_{17}$, but they are not layered compounds.

The most notable result was that Ni over $K_4Nb_6O_{17}$ had a very small peak intensity after every treatment compared with those of reference materials. The normalized intensities are summarized in Table 2. The intensity of Ni2$p_{3/2}$ including both main and satellite peaks was divided by that of Nb3d which consisted of 3$d_{5/2}$ and 3$d_{3/2}$ peaks. From Table 2, it is found that the peak intensity ratio of Ni2$p_{3/2}$/Nb3d for NiO(1 wt%)–$K_4Nb_6O_{17}$ is smaller by about 2 orders of magnitude than that for NiO(1 wt%)–$KNbO_3$ after every treatment. As XPS is sensitive only for surface region (20–30 Å in depth), the small values for NiO(1 wt%)–$K_4Nb_6O_{17}$ catalysts indicate that most of the loaded nickel locates inside of the catalyst where it is not detectable by XPS, while loaded nickel locates only at the surface in the case of $KNbO_3$. To estimate the degree of distribution of loaded nickel in $K_4Nb_6O_{17}$, the intensity ratio of Ni2$p_{3/2}$/Nb3$d_{5/2}$ was compared with the calculated value as shown in Table 3. For the calculation, 5.0 and 13.9 for Nb3$d_{5/2}$/C1s and

$Ni2p_{3/2}$/C1*s* were used, respectively, as relative cross sections of photoelectron emission by MgKα X-ray. The difference in the escape depths of photoelectrons between $Nb3d_{5/2}$ and $Ni2p_{3/2}$ was neglected. For the calculation of the untreated NiO(1 wt%)–$K_4Nb_6O_{17}$ catalyst, Ni atoms were assumed to be dispersed homogeneously in the interlayer spaces of $K_4Nb_6O_{17}$. The same procedure was also adopted to $NiNb_2O_6$ to estimate the accuracy of this calculation. The good agreement of experimental and calculated values both for $NiNb_2O_6$ and $K_4Nb_6O_{17}$ indicates that loaded nickel over $K_4Nb_6O_{17}$ is dispersed homogeneously in the interlayers of the catalyst during the impregnation.

XPS spectra of $Ni2p_{3/2}$ of NiO(1 wt%)–$K_4Nb_6O_{17}$ after various pretreatments are shown in Fig. 2. In the untreated catalyst, the nickel on the surface seems to exist as a mixture of NiO and $Ni(OH)_2$ as discussed previously (*13*). When the catalyst was treated by H_2 at 773 K (R773), most of the nickel was reduced to nickel metal at least within the region which is observable by XPS. When the catalyst was reoxidized at 473 or 773 K(R773-O473 or R773-O773 catalyst), surface nickel became NiO containing some excess oxygen.

The decrease in the intensity of $Ni2p_{3/2}$ after R773 and R773-O473 treatments compared with that of the untreated catalyst may be due to the aggregation of surface nickel to form Ni metal particles by these treatments. It should be emphasized that

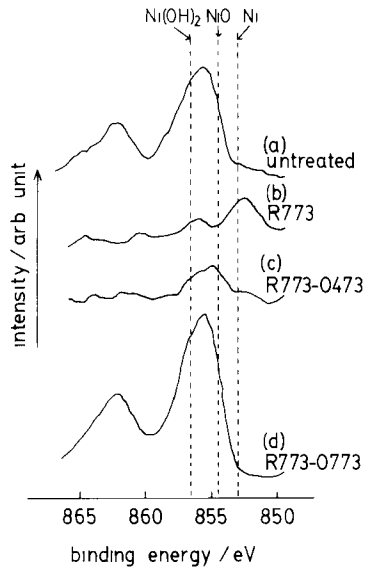

FIG. 2. XPS spectra of Ni $2p_{3/2}$ of NiO(1 wt%)–$K_4Nb_6O_{17}$ after pretreatments. (a) Untreated, (b) R773, (c) R773-O473, (d) R773-O773.

even after the pretreatments of R773 and R773-O473, the intensity of $Ni2p_{3/2}$ did not increase significantly and it is, therefore, concluded that most of the loaded nickel remains at the interlayers in active catalysts. When the reduced catalyst was reoxidized at the higher temperature (R773-O773), the intensity of $Ni2p_{3/2}$ increased compared with that reoxidized at the lower temperature (R773-O473). This fact suggests that the high temperature treatment by O_2 causes the segregation of nickel on the external surface of $K_4Nb_6O_{17}$ from the interlayer spaces. This was also confirmed by TEM as shown below.

TABLE 3

Comparison between Experimental and Calculated Values for XPS Peak Intensity Ratios of $Ni2p_{3/2}$/$Nb3d_{5/2}$

Catalyst	Ni/Nb[a]	$Ni2p_{3/2}/Nb3d_{5/2}$[b]	
		Calculated	Experimental
NiO(1 wt%)–$K_4Nb_6O_{17}$	1.45	0.06	0.04
$NiNb_2O_6$	1.2	1.4	1.0

[a] Ratio of the total numbers of Ni and Nb atoms.
[b] The calculation procedure is described in the text.

(3) *EXAFS*

The Fourier transforms of EXAFS functions $K^3\chi(K)$ for Ni *K* edge absorption of variously treated NiO–$K_4Nb_6O_{17}$ catalysts are shown in Fig. 3. The spectra of Ni foil (Ni–Ni, R = 2.47 Å, N = 12) and of NiO (Ni–Ni, R = 2.94 Å, N = 12; Ni–O, R = 2.09 Å, N = 6) prepared from $Ni(NO_3)_2$ by calcination at 973 K, which were taken as references to decide parameters for phase shift (polynominal) and amplitude functions

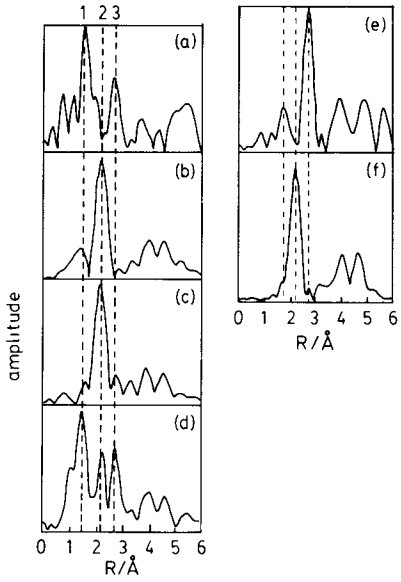

FIG. 3. Fourier transforms of Ni K edge EXAFS functions $K^3X(K)$ of NiO(1 wt%)–$K_4Nb_6O_{17}$ catalysts and references. Phase shift was not corrected. (a) Untreated, (b) R773, (c) R773-O473, (d) R773-O773, (e) NiO reference, (f) Ni metal reference. Interatomic distance 1 corresponds to Ni–O bond of NiO, 2 corresponds to Ni–Ni bond of Ni metal, and 3 corresponds to Ni–Ni of NiO.

(Lorentzian), are also shown in Fig. 3. Those parameters were used to analyze the data of sample catalysts and to determine bond length (R) and coordination numbers (N) for Ni–Ni and Ni–O of the catalysts. The bond lengths and the average coordination numbers are summarized in Table 4. In the case of the untreated catalyst, the peaks of Ni–O (R = 2.0 Å) and Ni–Ni (R = 2.98 Å) bonds corresponding to those of the NiO reference were observed as shown in Fig. 3a. The relative peak intensity of the Ni–Ni bond against that of Ni–O bond of the untreated catalyst was much smaller than that of the NiO reference in Fig. 3e. This indicates that the size of a "NiO-like" particle is very small in the untreated catalyst, probably several angstroms in diameter if a spherical shape is assumed. The average coordination number of Ni–Ni in Fig. 3a was ca. 5 while it was 12 for NiO in Fig. 3e. This again supports the conclusion that the size of "NiO-like" particles in $K_4Nb_6O_{17}$ is very small. Thus one can conclude that nickel loaded by the impregnation method followed by calcination exists as very small nickel oxide particles at the interlayers of $K_4Nb_6O_{17}$. This seems to be behavior similar to the formation of pillared clay materials in which small cluster ions such as $Ni_4(OH)_4^{4+}$ replace the cations at the interlayer spaces (*14*).

By the H_2 reduction at 773 K, the nickel in the catalyst was reduced completely to nickel metal as shown in Fig. 3b, in which the bond length of Ni–Ni (R = 2.48 Å) corresponds to that of nickel metal foil. In this process, H^+ must compensate the positive charge carried by Ni^{2+} ions. With rather large uncertainty, the average coordination number (N) of the first sphere in those Ni metal particles was estimated to be 8.0–10.7 which was obviously smaller than 12 of Ni foil. According to Greegor and Lytle (*15*), assuming the sphere particle of face-centered-cubic (fcc) packing, the particle size is estimated from the average coordination number N using the equation

$$r = \frac{a}{1.82}(N_T)^{1/3},$$

TABLE 4

Ni K Edge EXAFS Data of NiO(1 wt%)–$K_4Nb_6O_{17}$

Catalyst pretreatment	(NiO)				(Ni metal)		
	Ni–O		Ni–Ni		Ni–Ni		
	R(Å)	N	R(Å)	N	R(Å)	N	CS
Untreated[a]	2.01	2–3	2.98	3–5			
Untreated[b]	2.09	1	—	—			
R773					2.48	8–11	1st
					3.50	3–4	2nd
					4.27	12–13	3rd
					4.92	7–8	4th
R773-O473					2.50	7–9	1st
R773-O773	2.07	1–5	2.99	3–4	2.48	1–2	1st
NiO[c]	2.09	6	2.94	12			
Ni metal[c]					2.47	12	1st
					3.49	6	2nd
					4.28	24	3rd
					4.94	12	4th

Note R, interatomic distance between an absorber Ni atom and a scatterer atom, N, average coordination number of the sphere, CS, coordination sphere

[a] Prepared by the impregnation method

[b] Prepared by the ion-exchange method

[c] References.

where r is the radius of a metal particle (Å), a is the shortest interatomic distance (Å), and N_T is the total number of atoms in the particle.

For the nickel metal particle, a is 2.46 Å and N_T is evaluated from the coordination number (N) using Fig. 2 in Ref. *15*. For the R773 catalyst, N_T was 35–600 atoms. Thus the radius of the nickel metal particle is estimated to be 4.4–11.3 Å; i.e., the diameter of the particle is 8.8–22.6 Å. It is also possible to estimate the particle size from the number of the third coordination sphere. The diameter determined from the value is ca. 11.8 Å. In any case the particle size of Ni metal estimated from EXAFS data is considerably larger than the "interlayer I" spacing of 5.8 Å for $K_4Nb_6O_{17} \cdot 3H_2O$.

Shown in Fig. 3c is a Fourier transform of R773-O473 catalyst. R773-O473 catalyst which possibly contained a small amount of NiO was observed almost unchanged from R773 catalyst of Fig. 3b. The average coordination number (N) is also the same value as that of the R773 catalyst within the experimental error. On the other hand, the nickel detected by XPS was oxidized to NiO. Thus, by oxidation at 473 K, only the nickel on or close to the surface of $K_4Nb_6O_{17}$ was oxidized and most of the nickel in $K_4Nb_6O_{17}$ interlayers remained as nickel metal particles. When the catalyst was reoxidized at higher temperature, i.e., the R773-O773 catalyst, the major part of the nickel was oxidized to NiO although some nickel metal still remained as shown in Fig. 3d.

(4) TEM Observation

(a) NiO(1 wt%)–$K_4Nb_6O_{17}$ catalyst. To compare the TEM photographs with the results of XPS and EXAFS, TEM was studied not only for a 0.1-wt% NiO-loading catalyst but also for a 1-wt% NiO-loading catalyst, the activity of which was lower than that of 0.1-wt% NiO-loading catalyst. In Fig. 4, several photographs of NiO(1 wt%)–$K_4Nb_6O_{17}$ are shown. Fig. 4a is a micrograph of a sample reduced at 773 K. Ni metal particles of 30–150 Å are observed. It should be noted that such Ni particles were not so homogeneously dispersed for every $K_4Nb_6O_{17}$. Actually some $K_4Nb_6O_{17}$ particles carried more Ni particles than others. The sample used in Fig. 4a which contained more Ni metal particles than the average, is a typical example of this. Figure 5 shows NiO(1 wt%)–$KNbO_3$ reduced at 773 K. As mentioned above, $KNbO_3$ is not a layered material with particle size (1–10 μm) and BET surface area measured by N_2 (ca. 1 m^2/g) similar to those of $K_4Nb_6O_{17}$. It is clear that much more Ni metal particles 50–200 Å in diameter are observed on NiO(1 wt%)–$KNbO_3$ than on NiO(1 wt%)–$K_4Nb_6O_{17}$. Figure 4b shows the picture of the same sample in Fig. 4a taken from the direction parallel with the basal plane. Ni metal particles of 30–100 Å are observed to be dispersed over $K_4Nb_6O_{17}$. Yet, it is difficult to conclude from these micrographs whether the nickel particles are located at the surface of the $K_4Nb_6O_{17}$ or are buried in the lattice. Taking account of XPS results, at least some of the Ni metal particles must exist in the bulk of $K_4Nb_6O_{17}$ because the XP intensity of Ni2p over $K_4Nb_6O_{17}$ is ca. 1% of that of $KNbO_3$ as shown in Table 2. When the reduced sample was oxidized at 473 K, which gives more active photocatalyst, no significant change in the micrograph was observed. Oxidation at 773 K, however, caused a marked change in the loaded nickel as shown in Fig. 4c. This treatment resulted in a drastic decrease in photocatalytic activity. Rather large particles, which can probably be attributed to aggregated NiO(100–300 Å), were observed in this sample, in which small metallic Ni remained as shown by EXAFS (Fig. 3d).

(b) NiO(0.1 wt%)–$K_4Nb_6O_{17}$. This catalyst showed the highest activity for the photodecomposition of water, and there is a significant difference between the TEM photographs of a 0.1-wt% NiO-loading sample and that of a 1-wt% NiO-loading sample. Large Ni metal particles of 30–100 Å were scarcely observed for a 0.1-wt%

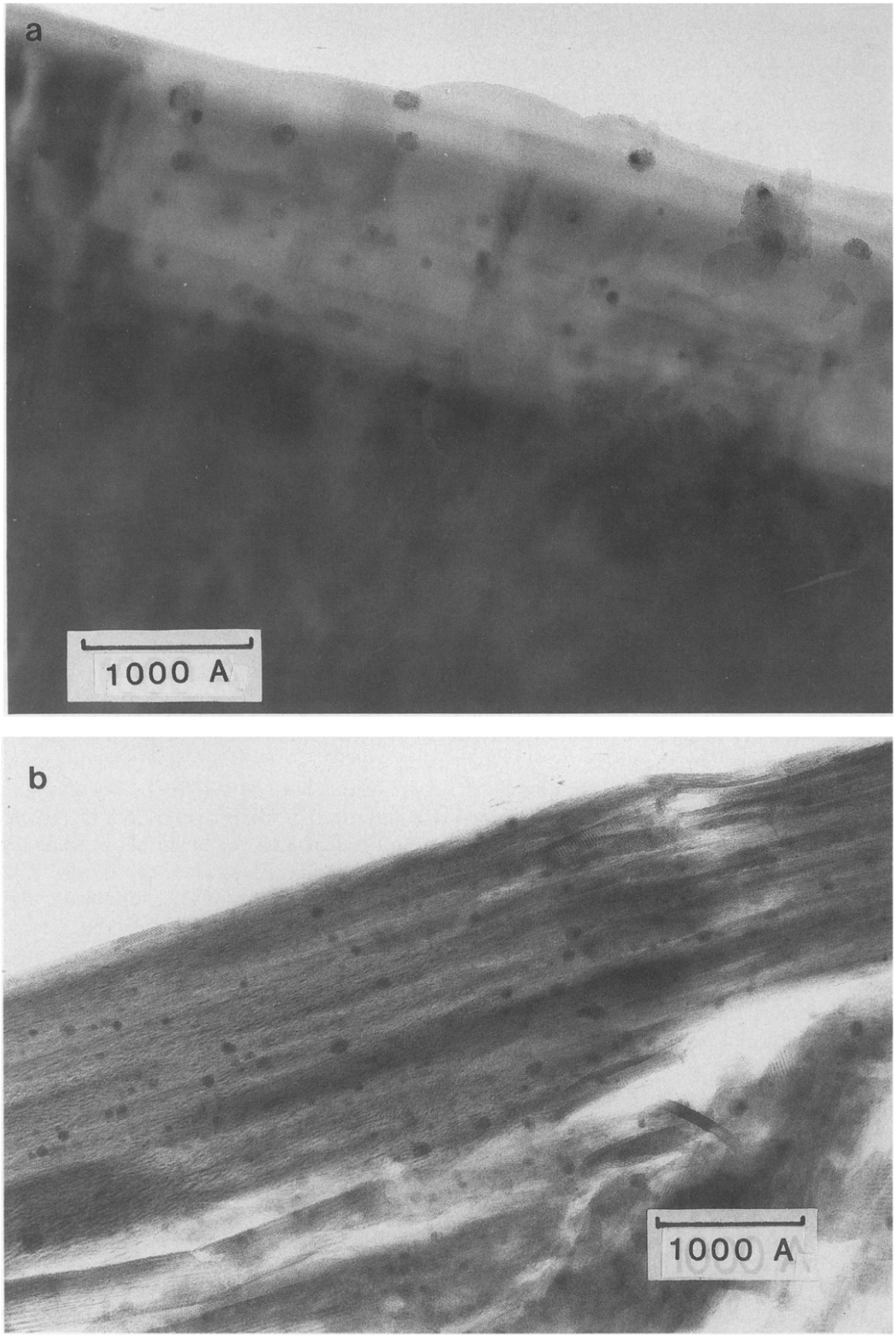

FIG. 4. TEM photographs of NiO(1 wt%)–$K_4Nb_6O_{17}$. (a) After R773 treatment taken from the direction perpendicular to the basal plane of $K_4Nb_6O_{17}$ by JEM-2000EX at 200 KV, ×257,600; (b) after R773 treatment taken from the direction parallel to the basal plane by JEM-2000EX at 200 KV, ×223,200; (c) after R773-O773 treatment by JEM-2000FX at 200 KV, ×342,000.

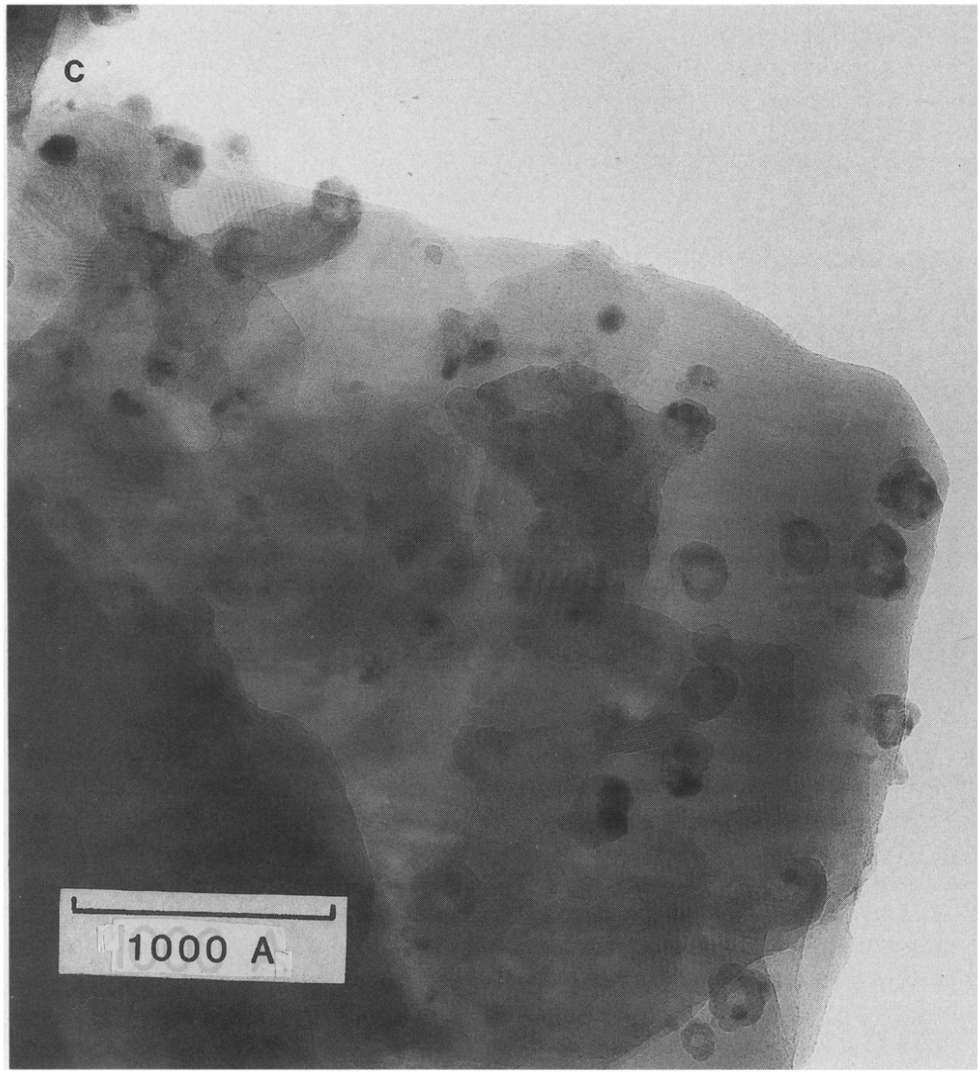

FIG. 4—*Continued.*

NiO–loading $K_4Nb_6O_{17}$ as shown in Fig. 6a. It looks like the same sample as $K_4Nb_6O_{17}$ itself at the low magnification shown in Fig. 6a (×152,000). When the micrograph is magnified much more (×3,237,000), one is barely able to distinguish a slight change in the depth of color in the $K_4Nb_6O_{17}$ lattice image as shown in Fig. 6b. After extensive work and careful examination we attributed the change in color to ultrafine Ni metal particles of ca. 5 Å. The Ni metal particles of less than 5 Å encapsulated in $K_4Nb_6O_{17}$, if they exist, would be difficult to identify by present TEM measurements. Therefore, it is not clear whether such small particles of less than 5 Å in diameter exist in $K_4Nb_6O_{17}$ or not. In any case, it is obvious that in a NiO(0.1 wt%)-loaded $K_4Nb_6O_{17}$ catalyst the loaded nickel exists as ultrafine particles of several angstrom order after R773 and R773-O473 treatments.

(5) *XRD*

The (040) reflection and the *b*-axis lengths of various NiO–$K_4Nb_6O_{17}$ catalysts were compared after R773-O473 treatment

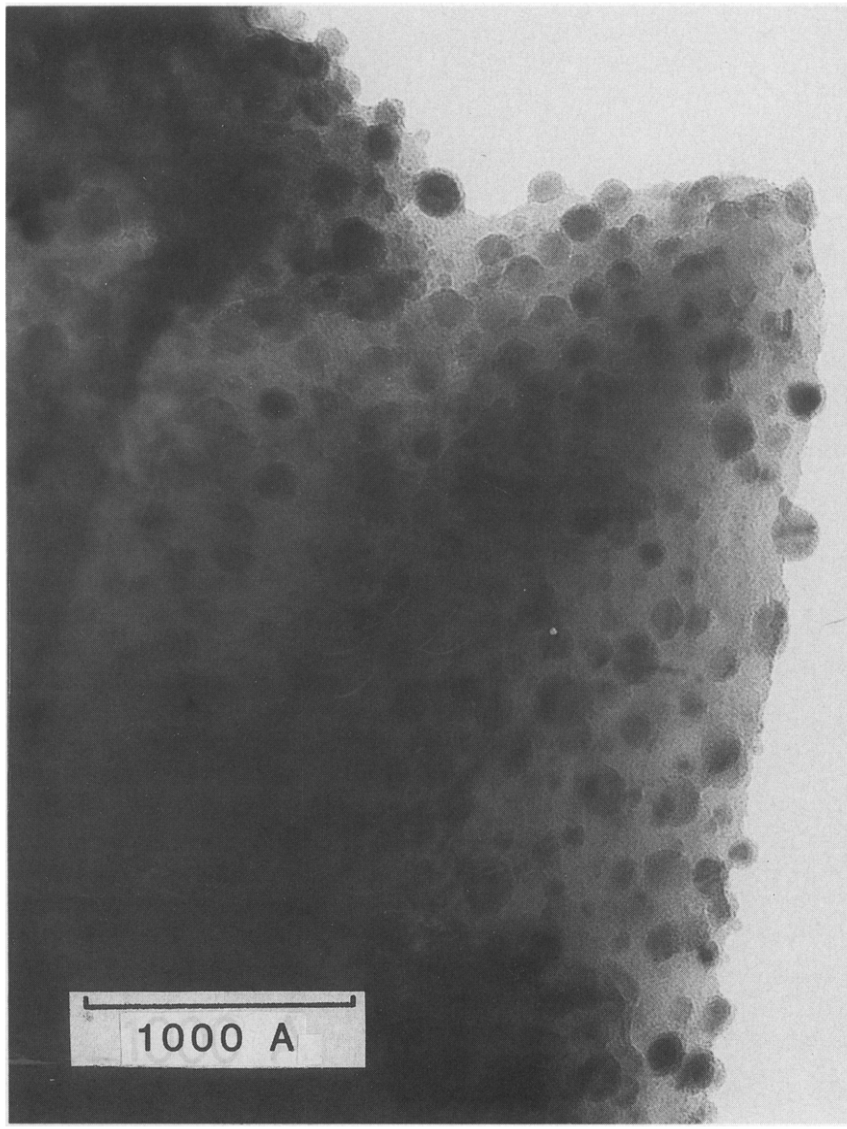

FIG. 5. TEM photograph of NiO(1 wt%)–$KNbO_3$ after R773 treatment by JEM-2000FX, ×160,000.

followed by hydration in air. Although the amount of the hydrated water for each nickel-loaded $K_4Nb_6O_{17}$ sample was not determined, the *b*-axis lengths were substantially identical for all samples, ca. 38 Å. No significant difference in XRD patterns was observed for NiO(0.1 wt%)–$K_4Nb_6O_{17}$ or NiO(1 wt%)–$K_4Nb_6O_{17}$ from that of $K_4Nb_6O_{17}$ itself while for NiO(20 wt%)–$K_4Nb_6O_{17}$ all peak intensities considerably decreased, which suggests the crystal structure of $K_4Nb_6O_{17}$ is broken to some extent.

DISCUSSION

(*1*) *Structure of Nickel-Loaded $K_4Nb_6O_{17}$ Photocatalyst*

From the results of XPS, EXAFS, TEM, and XRD studies, the structure of an active catalyst has become clear.

XPS revealed that for the NiO(1 wt%)–$K_4Nb_6O_{17}$ loaded nickel was predominantly located inside of $K_4Nb_6O_{17}$ and a small amount of nickel remained over the external surface. The same result is reasonably expected for the case of NiO(0.1 wt%)–$K_4Nb_6O_{17}$ catalyst.

According to Kinomura *et al.* (*11*), Ni^{2+} ions replace only the K^+ ions in interlayer I but not those in interlayer II during the ion exchange reaction at 363 K which is a temperature close to that of the impregnation method of the present work. Loaded nickel is, therefore, located predominantly in interlayer I. From the result of EXAFS in Fig. 3a, it is clear that the loaded nickel exists as small "NiO-like" particles after calcination in air at 573 K when the impregnation method applied. On the other hand, another type of NiO–$K_4Nb_6O_{17}$ catalyst was also prepared in an ion-exchange method similar to that of Kinomura *et al.* In this case Ni^{2+} ions seems to be dispersed atomically as shown in Table 4. After the R773 or R773-O473 treatment, both catalysts showed almost equal activities for the photodecomposition of water. Therefore, it is supposed that the difference between the two types of loaded Ni^{2+} forms does not affect the structure of the active catalyst after R773 or R773-O473 pretreatment.

When the catalyst was reduced at 773 K for 2 h, the loaded nickel which could be observed by EXAFS was completely reduced to Ni metal. At this stage of the catalyst treatment, TEM photographs manifested a significant difference between NiO(0.1 wt%)- and NiO(1 wt%)–$K_4Nb_6O_{17}$ catalysts. In NiO(1 wt%)–$K_4Nb_6O_{17}$ larger Ni metal particles 30–150 Å in diameter were observed as shown in Figs. 4a and 4b, while in NiO(0.1 wt%)–$K_4Nb_6O_{17}$ such large particles were scarcely observed even if the difference in the amounts of loaded Ni were taken into consideration. The particle size of Ni metal in NiO(1 wt%)–$K_4Nb_6O_{17}$ estimated from the coordination number of EXAFS is 8.8–22.6 Å, which is rather smaller than that observed by TEM in Figs. 4a and 4b. It should be noted that the coordination number obtained by EXAFS is the average value for all loaded Ni atoms. This discrepancy between EXAFS and TEM results, therefore, suggests the existence of Ni metal particles of much smaller size which are not observable in Figs. 4a and 4b. Actually in NiO(0.1 wt%)–$K_4Nb_6O_{17}$ ultrafine Ni metal particles of ca. 5 Å were perhaps barely observed as shown in Fig. 6b. The existence of ultrafine Ni metal particles of less than 5 Å was, however, not confirmed by the present experiment because of the resolution limit of the apparatus. From these results and considerations, it is reasonable to suppose that ultrafine Ni metal particles coexist with rather large Ni metal particles of 30–150 Å in NiO(1 wt%)–$K_4Nb_6O_{17}$. As the photocatalytic activity of NiO(0.1 wt%)–$K_4Nb_6O_{17}$ is higher by a factor of 2 than that of NiO(1 wt%)–$K_4Nb_6O_{17}$, it is concluded that the ultrafine particles of Ni metal are responsible for the photodecomposition of water. The interlayer spacing of $K_4Nb_6O_{17}$ (Nb–Nb distance across interlayer I along the *b* axis) is estimated to be ca. 6 Å although niobate sheets are corrugated. Therefore, one may suppose that most of the ultrafine Ni metal particles can be encapsulated in interlayer I without collapsing the layered structure. On the other hand, large Ni metal particles of 30–150 Å, if they exist in the internal space of $K_4Nb_6O_{17}$, must destroy the layered structure. Judging from XPS signal intensities of Ni 2*p* and the number of Ni metal particles observed by TEM photographs, we believe some of those large Ni metal particles locate inside of $K_4Nb_6O_{17}$, although no significant difference in XRD patterns was observed between NiO(1 wt%)–$K_4Nb_6O_{17}$ and $K_4Nb_6O_{17}$ itself. Large Ni metal particles incorporated in $K_4Nb_6O_{17}$ are considered to decrease the photocatalytic activity instead of working as active sites, which is also confirmed by the very low activity of NiO(20 wt%)–$K_4Nb_6O_{17}$ catalyst.

When the catalyst was reoxidized at 473 K, the Ni metal at the external surface of

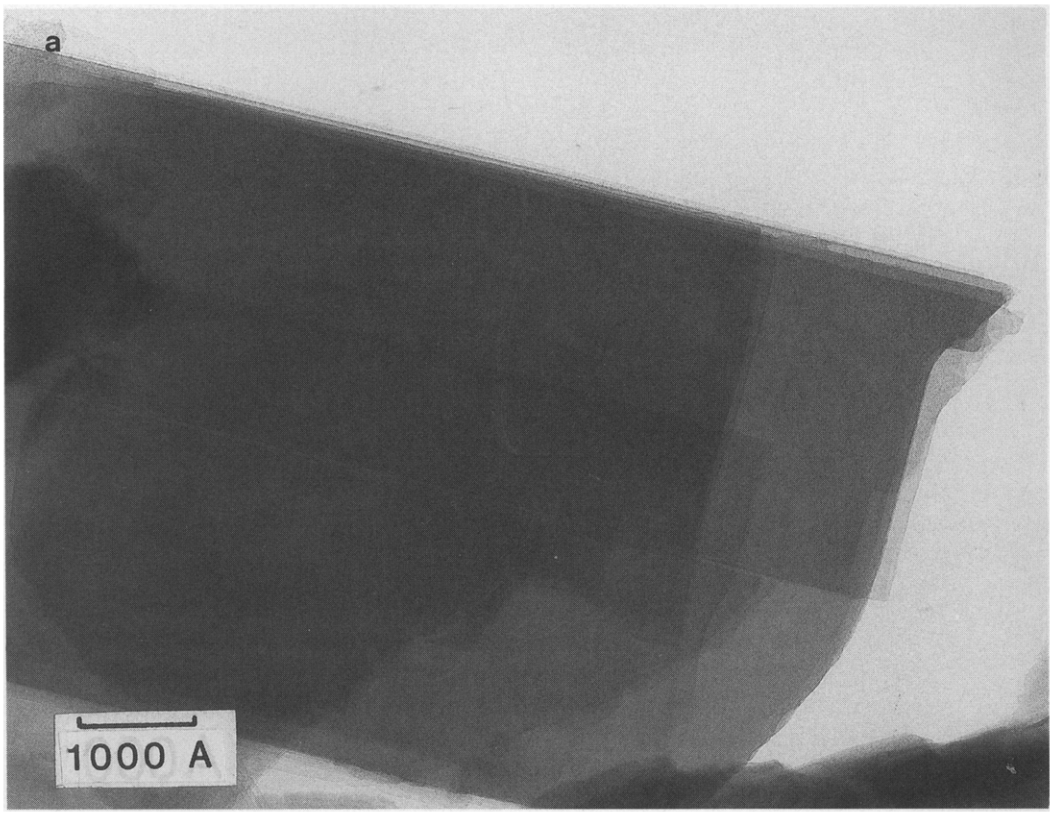

FIG. 6. TEM photographs of NiO(0.1 wt%)–$K_4Nb_6O_{17}$. (a) After R773 treatment by JEM-2000EX at 200 KV, ×152,000; (b) after R773 treatment by EM-002B/UHR at 200 KV. Some of the ultrafine nickel metal particles are indicated by arrows. ×3,237,000.

$K_4Nb_6O_{17}$ was reoxidized to NiO as determined from XPS results. The result of EXAFS in Fig. 3, however, showed that most of the Ni remained as Ni metal. Ni metal particles located at the interlayer space remained unchanged under O_2 oxidation at 473 K, which indicates the difficulty of migration of gaseous O_2 into the interlayer spacings. The higher activity of R773-O473 catalyst than that of R773 catalyst is probably due to the lack of Ni metal at the external surface of $K_4Nb_6O_{17}$ where the reverse reaction from H_2 and O_2 to form H_2O proceeds. The shortage of evolved O_2 over R773 NiO(1 wt%)–$K_4Nb_6O_{17}$ may be explained by the reaction that O_2 is consumed for the oxidation of Ni metal at the external surface. In the case of the reoxidation at higher temperature (R773-O773), the activity drops drastically as shown in Table 1. On the other hand, Ni metal particles encapsulated in $K_4Nb_6O_{17}$ were oxidized by the reoxidation at 773 K and some of those nickel particles migrated to the external surface out of the interlayer spacings to form large particles of NiO. Therefore, by this treatment the structure of an active catalyst for H_2O decomposition must be broken.

From the results discussed above it is obvious that the activity of the overall water splitting is very sensitive to the structure of the catalyst.

(2) *Mechanism for the Photocatalytic Decomposition of Water over Nickel-Loaded $K_4Nb_6O_{17}$*

Under the band gap irradiation (≥3.3 eV), niobate sheets absorb photons which produce electrons in the conduction band

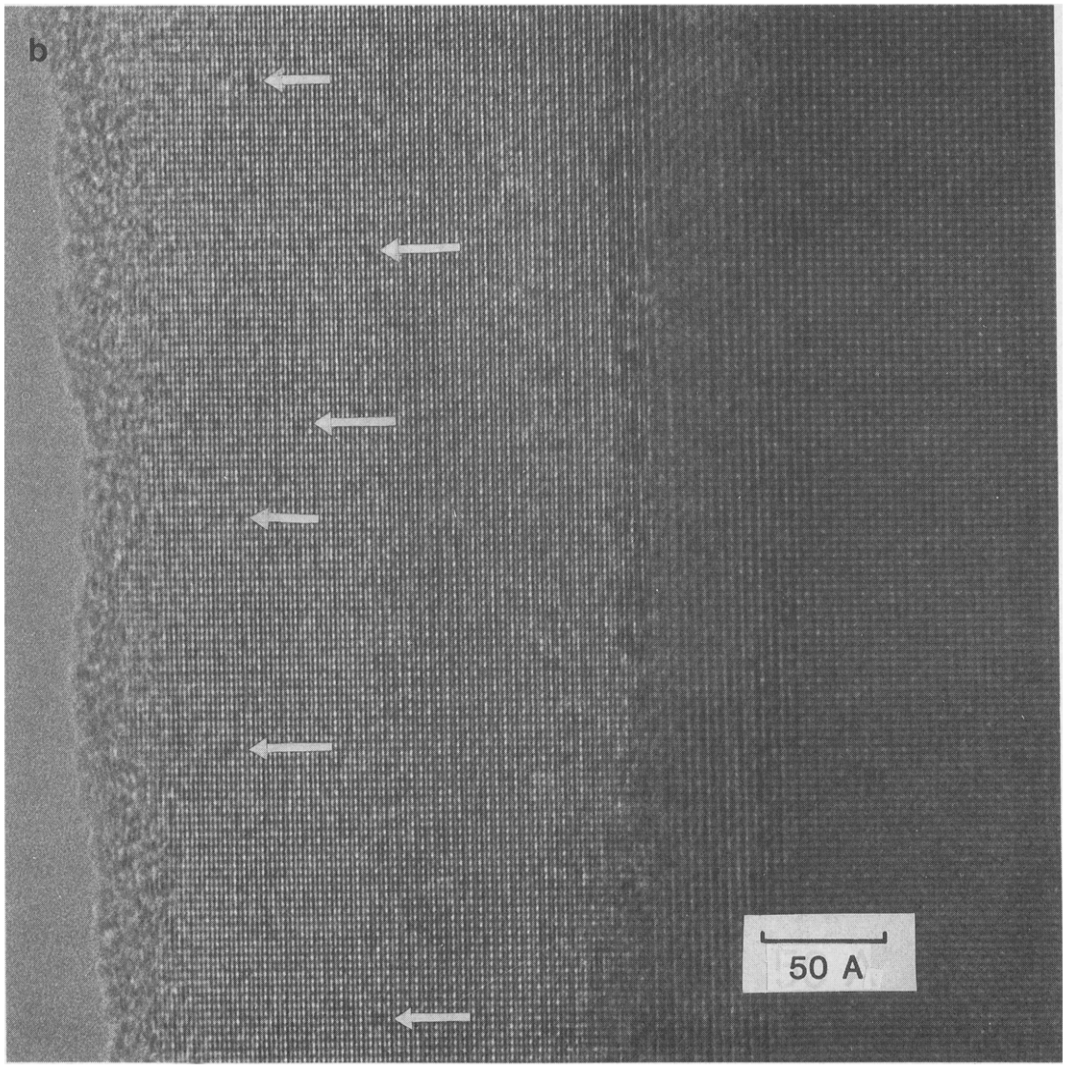

FIG. 6—*Continued.*

and holes in the valence band. The excited electrons and holes may be alternatively expressed as Nb^{4+} and O^- species. As each niobate sheet is separated from others by K^+ ions and hydrated water molecules, excited electrons and holes are unlikely to move through interlayer spaces. Therefore, this material is regarded as an accumulated "two dimensional" photocatalyst although niobate sheets are corrugated.

In our previous work (*3*, *5*), it has been suggested that loaded Ni metal particles facilitate the evolution of H_2. Therefore it is supposed that the ultrafine nickel metal particles at interlayer I can work as reduction sites to form H_2. Although $K_4Nb_6O_{17}$ itself has rather high ability to form H_2 as a photocatalyst (*5*), the nickel metal particles are expected to facilitate the formation of H_2. Another important aspect of the existence of nickel metal particles at interlayer I may be the clear separation of the reduction sites from the oxidation sites which are discussed below. If a homogeneous particle size (10 Ni atoms/particle) and a homogeneous dispersion of those particles are as-

sumed, a nickel metal particle exists every ca. 10,000 Å^2 (=100 Å × 100 Å) at interlayer I for NiO(0.1 wt%)–$K_4Nb_6O_{17}$, while a K^+ ion occupies 12.6 Å^2. The calculated turnover frequencies of H_2 formation on those particles are 70 molecules H_2/h/Ni-particle for 0.1 wt% NiO loading.

The sites of H_2 formation is identified rather clearly as discussed above, while those of O_2 production are not so obvious. For O_2 evolution, there seem to be three possible sites, i.e., (A) interlayer I, (B) interlayer II, and (C) edge plane. At the present stage, we do not have any conclusive results to identify the oxidation site. If H_2O oxidation proceeds at interlayer I, the sites should be close to Ni metal particles which work as the reduction sites. In our previous work on a NiO–$SrTiO_3$ photocatalyst (*3*), Ni–$SrTiO_3$ reduced at 773 K was found not to decompose water into H_2 and O_2 but to evolve only a small amount of H_2, and also the activity was found to decrease rapidly. In that case, nickel metal particles ca. 200 Å in diameter deposited on the $SrTiO_3$ surface and oxidized to form mainly $Ni(OH)_2$ under irradiation. Thus, it is also suspected for the present catalyst that the Ni metal particles at interlayer I are oxidized and the activity decays rapidly if the oxidation of water occurs mainly at interlayer I. Actually for NiO(0.1 wt%)–$K_4Nb_6O_{17}$ catalyst the oxidation of Ni metal particles was observed during the photodecomposition of water and it caused a decrease in activity (*5*). The oxidation rate of Ni metal particles was, however, very slow; i.e., it was less than 0.4% of the rate of O_2 evolution. Therefore, if model (A) is the case, the ultrafine Ni metal particles at interlayer I must be protected from oxidation by some unknown mechanism.

On the other hand, in model (B) each H_2 and O_2 is formed at opposite sides of a niobate sheet. The charge separation is accomplished by a membrane of an atomic order of thickness, and the products are automatically separated into two different parts without oxidation of nickel metal particles. One condition which should be proved to support this mechanism is the existence of enough intercalated water as a reactant at interlayer II. As mentioned above, while interlayer I is hydrated easily to form $K_4Nb_6O_{17} \cdot 3H_2O$ even in air, interlayer II is rather stable against hydration. Nevertheless, it was found that in distilled water the hydration number n is 4.5 or more and some K^+ ions (ca. 5% of total K^+ ions) are eluted and replaced by H^+ ions under the reaction conditions. According to the work of Kinomura *et al.* (*11*), interlayer II is hydrated as well as interlayer I when the K^+ ions are exchanged by smaller monovalent cations such as Na^+ and Li^+. Thus, under the reaction conditions in distilled water, it seems reasonable to expect the existence of some water molecules in interlayer II as a result of equilibrium between water molecules in the solution and in interlayer II. It is noteworthy that the decrease in the activity of the photodecomposition of water at high pH regions (>11) is explained by this model. According to the previous studies on TiO_2(4,6)- and $SrTiO_3$(2,3)-based photocatalysts, the activity of photodecomposition of water remarkably increased in concentrated NaOH or KOH solutions. On the other hand, for NiO-$K_4Nb_6O_{17}$ catalyst (*5*), the activity showed the maximum at pH ca. 11 and decreased markedly in more concentrated KOH solutions. Furthermore, at pH 14 a small amount of H_2 and no O_2 evolved. As the activity was recovered when the solution of concentrated KOH was replaced by distilled water, the low activity at high pH is not attributed to the degradation of the catalyst itself. In the case of model (B), the important factor would be the concentration of water at interlayer II, which may be controlled by the degree of replacement of K^+ by H^+ ions. Thus, it is inferred that the higher the concentration of KOH, the lower the amount of water at interlayer II. Accordingly, at very high concentrations of KOH, the amount of water molecules at interlayer II

is too small to sustain the photodecomposition of water with a high efficiency.

The driving force of the movement of electrons and holes might be provided by the electrostatic gradient in the niobate sheet, which is caused by different locations of cations K^+ and H^+ between interlayer I and II.

In the case of model (C), O_2 is produced on the edge plane, and evolves directly into the solution or into the gas phase. Ni metal particles at interlayer I are stable against O_2 oxidation, which was well demonstrated in Fig. 3C. The problem of this model is to find the driving force for the migration of holes to the edge plane. As the typical particle size of $K_4Nb_6O_{17}$ is 1–10 μm, holes must be transported considerably long distances within the corrugated niobate sheet. Although one may expect the band bending observed in such a case to be *n*-type semiconductor interface, this seems to be unlikely for this system because K^+ and H^+ ions and H_2O molecules are able to move throughout the bulk of $K_4Nb_6O_{17}$. Thus, the electrostatic field at the interface, if existent, would be effectively shielded by those ions.

It is, of course, possible that some of these models are operating simultaneously, especially model (A) and model (B). One of the supporting indication for O_2 formation at the interlayers as in model (A) and (B) is that the small but detectable amount of O_2 evolution continued for ca. 1 h even after irradiation ceased, while H_2 evolution stopped immediately. This may suggest the slow diffusion of O_2 from the interlayer to the outside. Another indication is the ESR signal observed in NiO(0.1 wt%)–$K_4Nb_6O_{17}$ after irradiation in distilled water. This species can probably be attributed to the O_3^- species, judging from the shape and the *g* value (g = 2.014), which is stable even in air for a long time. Such behavior is unusual for O_3^-, and it is inferred that the species is formed at the interlayer during the reaction.

Among the three models discussed above, we dare to put emphasis upon model (B) because it provides a novel mechanism for the charge separation in the photocatalyst. In Fig. 7, this mechanism is schematically depicted on the basis of the structure which is revealed in this study. Recently, Bard *et al.* also pointed out the advantage of the photocatalyst with an atomic order of thickness for the reason that long-distance diffusion of excited electrons and holes is avoided in such a system (*16*).

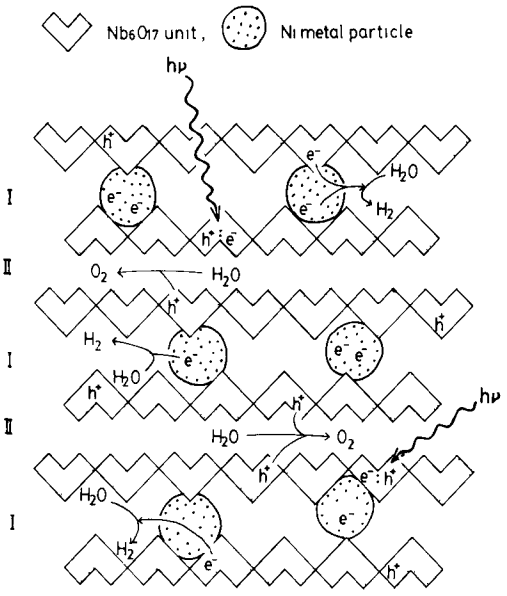

FIG. 7. Schematic structure of the active NiO(0.1 wt%)–$K_4Nb_6O_{17}$ photocatalyst and the reaction mechanism of H_2O decomposition into H_2 and O_2.

In this study, it has been proved that $K_4Nb_6O_{17}$ loaded with Ni metal particles is an accumulation of two-dimensional photocatalysts, i.e., niobate sheets with an atomic order of thickness (4 Å). Although further study is necessary to confirm the mechanism proposed in this work, various applications of this type of materials are conceivable.

SUMMARY

The structure of nickel-loaded $K_4Nb_6O_{17}$ powder, which is an active photocatalyst for an overall water splitting, was revealed by means of XPS, EXAFS, TEM, and XRD. $K_4Nb_6O_{17}$ is a layered compound which possesses two kinds of interlayer

spaces (interlayers I and II) alternately and K^+ ions at the interlayer spaces are exchanged for other cations. It is hydrated easily in water to form $K_4Nb_6O_{17} \cdot nH_2O$ (n = 4.5 or more). XPS showed that loaded nickel predominantly located at the interlayer spaces even after pretreatment. The nickel in an active photocatalyst was found to exist as Ni metal after R773 and R773-O473 treatment by EXAFS. Ultrafine Ni metal particles of ca. 5 Å were observed in NiO(0.1 wt%)–$K_4Nb_6O_{17}$ catalyst by TEM, while larger Ni metal particles of 30–150 Å also existed in NiO(1 wt%)–$K_4Nb_6O_{17}$ catalyst. As NiO(0.1 wt%)–$K_4Nb_6O_{17}$ showed higher activity, it is inferred that utlrafine Ni metal particles are responsible for the photodecomposition of water.

From these results it is concluded that an active nickel-loaded $K_4Nb_6O_{17}$ photocatalyst contains ultrafine Ni metal particles at interlayer I, which work as H_2 evolution sites. For the O_2 evolution sites, we suggest interlayer II, which is a different side from the H_2 evolution sites of niobate sheets. The unique structure and reaction mechanism are able to explain several characteristic behaviors of this catalyst.

In conclusion, nickel-loaded $K_4Nb_6O_{17}$ photocatalyst decomposes intercalated water into H_2 and O_2 at the interlayer spaces with high efficiency and is regarded as a "two-dimensional" photocatalyst.

ACKNOWLEDGMENTS

The authors thank JEOL and ABT members for their kind help in taking TEM photographs. We also gratefully acknowledge the critical reading of this manuscript by J. Kondo.

REFERENCES

1. For example, Gratzel, M. A., "Energy Resources through Photochemistry and Catalysis." Academic Press, New York, 1983.
2. Lehn, J. M., Sauvage, J. P., and Ziessel, R., *Nouv. J. Chim.* **4,** 623 (1980); Lehn, J. M., Sauvage, J. P., Ziessl, R., and Hilaire, L., *Isr. J. Chem.* **22,** 168 (1982).
3. Domen, K., Naito, S., Soma, M., Onishi, T., and Tamaru, K., *J. Chem. Soc. Chem. Commun.*, 543 (1980); Domen, K., Naito, S., Onishi, T., Tamaru, K., and Soma, M., *J. Phys. Chem.* **86,** 3657 (1982); Domen, K., Naito, S., Onishk, T., and Tamaru, K., *Chem. Phys. Lett.* **92,** 433 (1982); Domen, K., Kudo, A., and Onishi, T., *J. Catal.* **102,** 92 (1986).
4. Sato, S., and White, J. M., *Chem. Phys. Lett.* **72,** 83 (1980); Sato, S., and White, J. M., *J. Catal.* **69,** 128 (1981); Yamaguchi, K., and Sato, S., *J. Chem. Soc. Faraday Trans. 1* **81,** 1237 (1985).
5. Domen, K., Kudo, A., Shinozaki, A., Tanaka, A., Maruya, K., and Onishi, T. J., *Chem. Soc., Chem. Commun.*, 356 (1986). Kudo, A., Domen, K., Tanaka, A., Maruya, K., Aika, K., and Onishi, T., *J. Catal.* **111,** 67 (1988).
6. Kudo, A., Domen, K., Maruya, K., and Onishi, T., *Chem. Phys. Lett.* **133,** 517 (1987).
7. Gerischer, H., *Electroanal. Chem. Inter. Electrochem.* **58,** 263 (1975), and references therein.
8. Gerischer, H. J., *Phys. Chem.* **88,** 6096 (1984).
9. Gasperin, M., and Le Bihan, M. T., *J. Solid State Chem.* **33,** 83 (1980); **43,** 346 (1982).
10. Legaly, G., and Beneke, K. J., *Inorg. Nucl. Chem.* **38,** 1513 (1976).
11. Kinomura, N., Kumada, N., and Muto, F. J., *Chem. Soc. Dalton Trans.*, 2349 (1985).
12. Oyanagi, H., Matsushita, T., Ito, M., and Kuroda, H., *KEK Rep.*, 83–30 (1984).
13. Domen, K., Kudo, A., Onishi, T., Kosugi, N., and Kuroda, H. J., *Phys. Chem.* **90,** 292 (1986).
14. Kepert, D. L., *in* "Comprehensive Inorganic Chemistry" (J. C. Bailer *et al.*, Eds.), Vol. 4, p. 607. Pergamon Press, Oxford, 1973.
15. Greegor, R. B., and Lytle, F. W., *J. Catal.* **63,** 476 (1980).
16. Leland, J. K., and Bard, A. J., *Chem. Phys. Lett.* **139,** 453 (1987).